CONSTANT-BEAMWIDTH LINEARLY CONSTRAINED MINIMUM VARIANCE BEAMFORMER

Ariel Frank Assaf Ben-Kish Israel Cohen
Andrew and Erna Viterbi Faculty of Electrical & Computer Engineering
Technion–Israel Institute of Technology, Haifa 3200003, Israel
{arielfrank@campus, assafbk@campus, icohen@ee}.technion.ac.il

***Abstract*—In this paper, we propose a new and flexible method for designing a constant-beamwidth beamformer that maintains directional constraints. We decompose the problem by designing a linearly constrained minimum variance beamformer and a constant-beamwidth beamformer based on the window technique. Subsequently, we utilize Kronecker product beamforming to merge the two elementary beamformers. While a competing method restricts the beamwidth depending on the interelement spacing and number of sensors in the array, the proposed method enables a flexible design of an arbitrary beamwidth. Experimental results demonstrate the improved performance of the proposed approach compared to the competing method. Specifically, the proposed beamformer achieves the desired beamwidth and directional constraints with a significantly higher directivity factor and lower sidelobe levels.**

***Index Terms*—Linearly constrained minimum variance (LCMV) beamformer, broadband beamformer, constant-beamwidth beamformer, Kronecker product, microphone array.**

I. Introduction

Broadband beamforming is useful in various fields, including audio, communication, and radar [1]–[3]. A frequency-invariant beampattern avoids signal distortion when the beampattern is not steered to the precise direction of the desired source. Blocking of directional interferences can be generally accomplished by designing the beampattern with nulls directed toward the interfering sources. Over the past few decades, constant-beamwidth beamforming has attracted much attention [4]–[7].Long et al. [8] introduced the window technique, where the window parameters are tuned per frequency to maintain a constant beamwidth. Their technique achieves high white noise gains (WNG) and directivity factors (DF) without sacrificing computational efficiency.

The linearly constrained minimum variance (LCMV) beamformer [9], [10] minimizes the variance of the beamformer output while maintaining directional constraints. A drawback of the LCMV beamformer is the need to invert a large and sometimes ill-conditioned covariance matrix. Wolff et al. [11] address this drawback by recursively computing the LCMV beamformer's weights (a smaller matrix is inverted at each stage). The generalized sidelobe canceller (GSC) [12] eliminates the need for matrix inversion by iteratively producing a beamformer that is equivalent to the LCMV beamformer [13]. The GSC consists of two beamformers that operate on orthogonal subspaces. One beamformer ensures that the linear constraints are satisfied while the other adaptively filters out the remaining noise. Currently, LCMV beamformers lack a straightforward method for achieving a constant beamwidth, and the constant-beamwidth beamformer proposed by Long et al. [8] fails to incorporate directional constraints.

Koh and Weiss [14] proposed modifying the linear constraints of the GSC, in addition to harmonic nesting and spatial tapering [15], to attain a constant beamwidth. Unfortunately, their method is limited in that the beamwidth is fixed at a value that depends on the number of sensors in the array and the spacing between them. The interelement spacing is set to half of the highest wavelength and is not adjusted to control the beamwidth. Moreover, the interferers' directions and noise affect the beamwidth due to the beamformer operating on the noise subspace.

This paper introduces a new and flexible method for designing a constant-beamwidth LCMV beamformer. We separately design a constant-beamwidth beamformer using the window technique and an LCMV beamformer that satisfies the directional constraints. Then we merge the two beamformers using generalized Kronecker product beamforming [16] to produce a constant-beamwidth LCMV beamformer. Compared to Koh and Weiss's beamformer [14], the proposed beamformer can be configured to have an arbitrary beamwidth and has superior DF and sidelobe levels but has marginally lower WNG.

II. Signal Model and Background

Consider a uniform linear array (ULA) with M omnidirectional sensors and interelement spacing of δ. We assume a far-field scenario in an anechoic environment: a plane wave arrives from the azimuth angle θ, $0^\circ \leq \theta \leq 180^\circ$, and propagates at the speed of sound in the air, $c = 343$ m/s. Using vector notation in the frequency domain, the measured signal at frequency f is given by

$$\mathbf{y}(f) = \mathbf{d}(f, \theta_{\mathrm{d}}) X(f) + \mathbf{v}(f)\,, \tag{1}$$

where $X(f)$ is the desired signal arriving from the direction θ_{d}, $\mathbf{v}(f)$ is the additive noise vector of length M, and $\mathbf{d}(f, \theta)$ is the steering vector of length M given by

$$\mathbf{d}(f, \theta) = \begin{bmatrix} 1 & e^{-\jmath u} & e^{-\jmath 2u} & \dots & e^{-\jmath (M-1)u} \end{bmatrix}^T , \tag{2}$$

where $u = \frac{2\pi f}{c} \delta \cos(\theta)$, $\jmath = \sqrt{-1}$, and ^{T} denotes transpose.

This work was supported by the Pazy Research Foundation.

Beamforming is performed by applying a linear spatial filter to the measured signal vector:

$$Z(f) = \mathbf{h}^H(f)\,\mathbf{y}(f)\,, \tag{3}$$

where $Z(f)$ is the beamformer's output, $\mathbf{h}(f)$ is the beamforming weight vector of length M, and ^{H} denotes conjugate transpose. The distortionless constraint,

$$\mathbf{h}^H(f)\mathbf{d}(f,\theta_{\mathrm{d}}) = 1\,, \tag{4}$$

normalizes the beamformer's weights to attain a frequency-invariant gain toward the direction θ_{d}. The beampattern is defined as the beamformer's response to a plane wave arriving from the direction θ:

$$\mathcal{B}[f,\theta,\mathbf{h}(f)] = \mathbf{d}^H(f,\theta)\mathbf{h}(f)\,. \tag{5}$$

The first null beamwidth (FNBW), $b(f)$, is the difference between the angles nearest to the mainlobe at which the value of the beampattern equals zero. With constant-beamwidth beamforming, the FNBW does not vary with frequency, i.e., $b(f) \equiv \theta_{\mathrm{B}}$, where θ_{B} denotes the desired FNBW. The sidelobe level is defined as the beampattern's maximum value over directions outside the mainlobe.

In this work, we steer the beamformer to the broadside direction, i.e., $\theta_{\mathrm{d}} = 90°$. We omit the variable f from now onward for conciseness.

A. LCMV Beamformer

Assuming that the desired signal and additive noise are statistically independent, the variance of Z is given by

$$\phi_Z = \phi_X \left|\mathbf{h}^H\mathbf{d}(\theta_{\mathrm{d}})\right|^2 + \mathbf{h}^H\mathbf{\Phi_v}\mathbf{h}\,, \tag{6}$$

where ϕ_X is the variance of X and $\mathbf{\Phi_v}$ is the covariance matrix of $\mathbf{v}$. The LCMV beamformer minimizes the noise component of (6) under N_{C} linear constraints:

$$\mathbf{h}_1 = \underset{\mathbf{h}}{\operatorname{argmin}}\,\mathbf{h}^H\mathbf{\Phi_v}\mathbf{h} \quad \text{s.t.} \quad \mathbf{C}^H\mathbf{h} = \mathbf{q}\,, \tag{7}$$

where $\mathbf{C}$ is a constraint matrix of size $M \times N_{\mathrm{C}}$ and $\mathbf{q}$ is a vector of length N_{C}. The solution to (7) is given by:

$$\mathbf{h}_1 = {\mathbf{\Phi_v}}^{-1}\mathbf{C}\left(\mathbf{C}^H{\mathbf{\Phi_v}}^{-1}\mathbf{C}\right)^{-1}\mathbf{q}\,, \tag{8}$$

which requires inverting an $M \times M$ covariance matrix $\mathbf{\Phi_v}$, which may sometimes be ill-conditioned.

We provide an example to demonstrate properties of the LCMV beamformer for a ULA with $M = 13$ sensors and interelement spacing $\delta = 3.2$ cm in the presence of white noise, i.e., $\mathbf{\Phi_v} = \mathbf{I}_M$, where $\mathbf{I}_M$ is the $M \times M$ identity matrix. The matrix $\mathbf{C}$ includes null constraints for $\theta_1 = 60°$ and $\theta_2 = 130°$ and distortionless constraint (4) for $\theta_{\mathrm{d}} = 90°$. The resulting LCMV beamformer is illustrated in Fig. 1(a). The LCMV beamformer exhibits high sidelobe levels at all frequencies (≈ -13 dB), and its FNBW is frequency-dependent (becomes narrower as the frequency increases). It is generally impossible to make the FNBW constant by adding constraints on the beampattern's amplitude. For example, naively adding two null constraints toward directions $\theta_{\mathrm{d}} \pm \frac{\theta_{\mathrm{B}}}{2}$ does not achieve a constant FNBW of $\theta_{\mathrm{B}} = 36°$ because other nulls fall between the added nulls, as seen in Fig. 1(b).

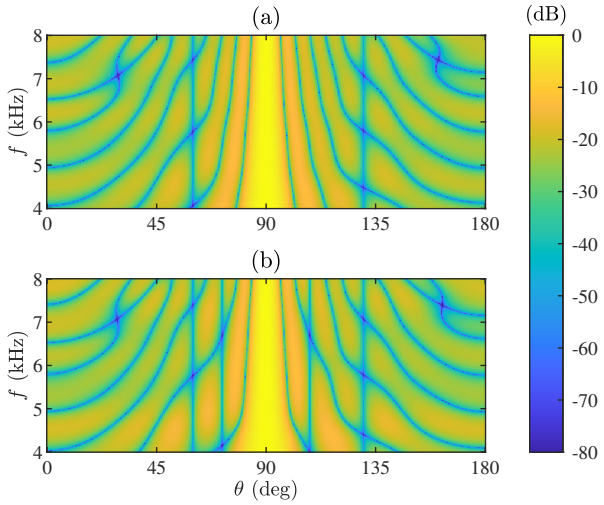

Fig. 1. LCMV beampatterns for $M = 13$, $\delta = 3.2$ cm, $\theta_{\mathrm{d}} = 90°$, and null constraints toward directions $\theta_1 = 60°$ and $\theta_2 = 130°$. In the lower plot, there are additional two null constraints toward directions $\theta_{\mathrm{d}} \pm \frac{\theta_{\mathrm{B}}}{2}$ for a desired FNBW of $\theta_{\mathrm{B}} = 36°$.

B. Constant-Beamwidth Beamformer

Long et al. [8] introduced a window-based technique to attain the beamwidth constancy. The main idea was to apply different shapes of windows for different frequency bins as real weighting coefficients of microphones. The beamwidth was maintained constant by controlling the window parameters. For example, we can use the Kaiser window [17],

$$w[m] = \frac{I_0\left[\beta\sqrt{1-\left(\frac{2m}{M-1}-1\right)^2}\right]}{I_0[\beta]}\,, \quad 0 \le m \le M-1\,, \tag{9}$$

which is easy to compute and gives near-optimal sidelobe attenuation for a given mainlobe width. Here, $I_0(x)$ is the zero-order modified Bessel function of the first kind, and β is the window shape factor, which represents the tunable parameter. Per frequency, the value of β is modified so that $b(f) \equiv \theta_{\mathrm{B}}$. To satisfy (4) for $\theta_{\mathrm{d}} = 90°$, the beamformer weights are further normalized:

$$h[m] = \frac{w[m]}{\sum_{m'=0}^{M-1} w[m']}\,, \quad 0 \le m \le M-1\,, \tag{10}$$

where $h[m]$ denotes the mth element of $\mathbf{h}$.

C. Kronecker Product Beamformer

Kronecker Product beamforming [18] is a flexible, simple, and robust technique for designing beamformers. The main idea is to decompose the physical array into subarrays, and design or optimize the subarrays separately.

Consider a ULA with $M = M_1M_2$ sensors and interelement spacing δ. This array is termed the physical array. The physical array's steering vector and beamforming weight vector, of lengths M, are denoted by $\mathbf{d}(\theta)$ and $\mathbf{h}$. Assume that we

decompose the physical array into two subarrays of sizes M_1 and M_2, such that

$$\mathbf{d}(\theta) = \mathbf{d}_1(\theta) \otimes \mathbf{d}_2(\theta)\,, \tag{11}$$

where $\mathbf{d}_1(\theta)$ denotes a steering vector of size M_1 for the first subarray, $\mathbf{d}_2(\theta)$ denotes a steering vector of size M_2 for the second subarray, and $\otimes$ is the Kronecker product. Then, we can design beamformers $\mathbf{h}_1$ and $\mathbf{h}_2$ for the subarrays, and apply the beamformer

$$\mathbf{h} = \mathbf{h}_1 \otimes \mathbf{h}_2 \tag{12}$$

to the physical array. As a result, the beampatterns of the subarrays, $\mathcal{B}(\theta, \mathbf{h}_i) = {\mathbf{d}_i}^H(\theta)\mathbf{h}_i$, $i \in \{1, 2\}$, are related to the beampattern of the physical array by a multiplication [18]:

$$\begin{aligned}\mathcal{B}(\theta, \mathbf{h}) &= \mathbf{d}^H(\theta)\mathbf{h} \\ &= \left[\mathbf{d}_1(\theta) \otimes \mathbf{d}_2(\theta)\right]^H (\mathbf{h}_1 \otimes \mathbf{h}_2) \\ &= \left[{\mathbf{d}_1}^H(\theta)\mathbf{h}_1\right]\left[{\mathbf{d}_2}^H(\theta)\mathbf{h}_2\right] \\ &= \mathcal{B}(\theta, \mathbf{h}_1)\mathcal{B}(\theta, \mathbf{h}_2)\,.\end{aligned} \tag{13}$$

III. Constant-Beamwidth LCMV Beamformer

In this section, we propose a novel method for designing a constant-beamwidth LCMV beamformer by separately designing LCMV and constant-beamwidth beamformers for two subarrays, and then joining them together with the Kronecker product beamforming method.

A. Physical Array Beampattern

Assume that N_I interferers impinge on the array from directions θ_i, $1 \le i \le N_\mathrm{I}$, outside of the desired mainlobe: $|\theta_i - \theta_\mathrm{d}| > \frac{\theta_\mathrm{B}}{2}$, $1 \le i \le N_\mathrm{I}$. Our goal is to design a beampattern with nulls in the interferers' directions while maintaining the distortionless constraint (4) and a constant FNBW of θ_B. Our design is for a ULA with M sensors and interelement spacing δ, but can be generalized to other array geometries. Using the terminology introduced in the previous section, this array is termed the physical array. We construct two subarrays of sizes M_1 and M_2, with interelement spacing δ, such that $M_1 + M_2 - 1 = M$ ($\neq M_1 M_2$). For this choice of subarrays, (11) does not hold. Examine the following steering vector of length $M_1 M_2$:

$$\overline{\mathbf{d}}(\theta) = \mathbf{d}_1(\theta) \otimes \mathbf{d}_2(\theta) \;\; [\neq \mathbf{d}(\theta)]\;. \tag{14}$$

The array that corresponds to this steering vector is termed the virtual array. We design beamformers $\mathbf{h}_1$ and $\mathbf{h}_2$ for the subarrays, and apply the beamformer

$$\overline{\mathbf{h}} = \mathbf{h}_1 \otimes \mathbf{h}_2 \tag{15}$$

to the virtual array. Similar to (13), the beampatterns of the subarrays are related to the beampattern of the virtual array, $\mathcal{B}(\theta, \overline{\mathbf{h}}) = \overline{\mathbf{d}}^H(\theta)\overline{\mathbf{h}}$, by a multiplication [16]:

$$\mathcal{B}(\theta, \overline{\mathbf{h}}) = \mathcal{B}(\theta, \mathbf{h}_1)\mathcal{B}(\theta, \mathbf{h}_2)\,. \tag{16}$$

Notice that the virtual array's steering vector contains the same values as the physical array's steering vector but in a different order and with some repetitions. They contain the same values because we set the subarrays' interelement spacing to δ and $M_1 + M_2 - 1 = M$. Denote by σ the permutation of the steering vectors, i.e., $\sigma\left[\mathbf{d}(\theta)\right] = \overline{\mathbf{d}}(\theta)$. Therefore, the virtual array's beampattern is equivalent to $\sigma\left[\mathbf{d}(\theta)\right]^H\overline{\mathbf{h}}$. Generalized Kronecker product beamforming [16] is performed by applying the virtual array's beamforming weight vector to the permutation of the physical array's measured signal vector:

$$Z = \overline{\mathbf{h}}^H \sigma\left(\mathbf{y}\right)\,, \tag{17}$$

which produces the same beampattern as the virtual array.

We show an alternative procedure for achieving the same beampattern. Instead of rearranging (with repetitions) the outputs of the physical ULA's sensors and then multiplying them with the virtual array's beamforming weights (17), we calculate an equivalent weight for each physical sensor. Formally, we seek for $\mathbf{h}$ that satisfies:

$$\forall\theta \in [0^\circ, 180^\circ]\colon\; \overline{\mathbf{d}}^H(\theta)\overline{\mathbf{h}} = \mathbf{d}^H(\theta)\mathbf{h}\,. \tag{18}$$

Proposition. *A solution to (18) is the linear convolution of the two subarrays' weights:*

$$h[m] = \sum_{k=k_1(m)}^{k_2(m)} h_1[k]h_2[m-k]\,,\quad 0 \le m \le M-1\,, \tag{19}$$

where $k_1(m) = \max(0,\, m + 1 - M_2)$ *and* $k_2(m) = \min(m,\, M_1 - 1)$.

Proof.

$$\begin{aligned}\overline{\mathbf{d}}^H(\theta)\overline{\mathbf{h}} &= \left[{\mathbf{d}_1}^H(\theta)\mathbf{h}_1\right]\left[{\mathbf{d}_2}^H(\theta)\mathbf{h}_2\right] \\ &= \left(\sum_{i=0}^{M_1-1} h_1[i]x^i\right)\left(\sum_{j=0}^{M_2-1} h_2[j]x^j\right) \\ &= \sum_{m=0}^{M_1+M_2-2}\;\sum_{k=k_1(m)}^{k_2(m)} h_1[k]h_2[m-k]x^m \\ &= \sum_{m=0}^{M-1} h[m]e^{jmu} \\ &= \mathbf{d}^H(\theta)\mathbf{h}\,,\end{aligned} \tag{20}$$

where $x \doteq e^{ju}$ and the third equality follows from the Cauchy product of two polynomials. ■

Next, we design the virtual array's beampattern. Once the beamformers of the subarrays, $\mathbf{h}_1$ and $\mathbf{h}_2$, are obtained, the beamformer of the physical array is obtained by (19). As a result, the virtual and physical arrays have the same beampatterns.

B. Virtual Array Beampattern

We can deduce from (16) that for directions in which one of the subarrays' beampatterns has a null, the virtual array's beampattern also has a null. Furthermore, designing both

subarrays to maintain (4), the virtual array would also maintain the distortionless constraint. For $\theta \neq \theta_{\rm d}$, the subarrays' beampattern's amplitudes should be less than 1. Therefore, for $\theta \neq \theta_{\rm d}$, the virtual array's beampattern's amplitude is less than each subarray's beampattern's amplitude. In other words, the sidelobe level of the virtual array is better than that of each subarray. Therefore, it is sufficient to design one subarray with high sidelobe attenuation. This is achieved by designing a subarray using the window technique. The other subarray is designed to have nulls in the interferers' directions and no nulls in the mainlobe.

To manage the interferers, consider a ULA with M_1 sensors and interelement spacing δ. This array is termed the LCMV subarray. To maintain the distortionless constraint (4) and block the interferers, we have $N_{\rm C} = N_{\rm I} + 1$ constraints given by

$$\mathbf{C}^H \mathbf{h}_1 = \mathbf{q}\,, \tag{21}$$

where

$$\mathbf{C} = \begin{bmatrix} \mathbf{d}_1(\theta_{\rm d}) & \mathbf{d}_1(\theta_1) & \mathbf{d}_1(\theta_2) & \dots & \mathbf{d}_1(\theta_{N_{\rm I}}) \end{bmatrix} \tag{22}$$

and

$$\mathbf{q} = \begin{bmatrix} 1 & 0 & 0 & \dots & 0 \end{bmatrix}^T . \tag{23}$$

Here, the dimensions of $\mathbf{C}$ are $M_1 \times N_{\rm C}$. To fulfill these directional constraints, an array of at least $N_{\rm C}$ sensors is required. We do not use more sensors so that the LCMV subarray's beampattern does not have nulls besides those at the interferers' directions. Otherwise, a null might be produced in the mainlobe. Additional benefits of limiting the number of sensors are providing more sensors to the second subarray (improving the sidelobe levels) and inverting a smaller covariance matrix to attain the subarray's weights. Therefore, we set $M_1 = N_{\rm C}$.

The LCMV subarray's beamforming weights are given by (8) (substituting (22) for $\mathbf{C}$, (23) for $\mathbf{q}$, and the subarray's noise covariance matrix of size $M_1 \times M_1$ is taken as the first M_1 rows and columns of $\mathbf{\Phi_v}$) producing the beampattern: $\mathcal{B}(\theta, \mathbf{h}_1) = {\mathbf{d}_1}^H(\theta)\mathbf{h}_1$, with values:

$$\mathcal{B}(\theta, \mathbf{h}_1) = \begin{cases} 1 & , \quad \theta = \theta_{\rm d}\,, \\ 0 & , \quad \theta \in \{\theta_i\}_{i=1}^{N_{\rm I}}\,. \end{cases} \tag{24}$$

Next, we design a constant-beamwidth beamformer with an FNBW of $\theta_{\rm B}$ for a ULA with $M_2 = M - M_1 + 1$ sensors and interelement spacing δ following the window technique outlined in Section II-B (replacing M with M_2 in (9) and (10)). This array is termed the CBW subarray. The designed beampattern is given by $\mathcal{B}(\theta, \mathbf{h}_2) = {\mathbf{d}_2}^H(\theta)\mathbf{h}_2$. By the constant-beamwidth design:

$$\mathcal{B}(\theta, \mathbf{h}_2) = \begin{cases} 1 & , \quad \theta = \theta_{\rm d}\,, \\ 0 & , \quad \theta = \theta_{\rm d} \pm \frac{\theta_{\rm B}}{2}\,. \end{cases} \tag{25}$$

The virtual array is subsequently produced from the two subarrays. It follows from (16), (24), and (25) that the virtual array's beampattern fulfills all design goals: a constant FNBW of $\theta_{\rm B}$, distortionless constraint for $\theta_{\rm d}$, and nulls toward the $N_{\rm I}$ interferers. The physical array's beamformer is obtained as a linear convolution of the two subarrays' beamformers using (19), producing a beampattern identical to that of the virtual array. Our design offers a tradeoff between the beamwidth and sidelobe levels. Increasing the FNBW specification improves the sidelobe levels since we use the Kaiser window for the CBW subarray's weights. Furthermore, the LCMV subarray's weights are produced by inverting a smaller $M_1 \times M_1$ covariance matrix compared to an $M \times M$ matrix.

IV. Experimental Results

In this section, we compare our proposed beamformer to Koh and Weiss's [14] for a ULA with $M = 13$ sensors in the presence of white noise, i.e., $\mathbf{\Phi_v} = \mathbf{I}_M$. The design requirements were to maintain an FNBW of $\theta_{\rm B} = 36^\circ$ over the frequency octave $[4, 8]$ kHz while maintaining the distortionless constraint and nulling interferers from $N_{\rm I} = 2$ directions: $\theta_1 = 60^\circ$ and $\theta_2 = 130^\circ$. The design can be extended to multiple octaves by using harmonic nesting [15].

For our proposed method, $M_1 = N_{\rm C} = 3$ and an interelement spacing of 3.2 cm was used. To reproduce Koh and Weiss [14], the interelement spacing was set to half of the highest wavelength, i.e., $\frac{1}{2}\frac{c}{8000} \approx 2.1$ cm. The constant-beamwidth GSC was reformulated as an LCMV by replacing the distortionless constraint with

$$\mathbf{c}^H \mathbf{h} = 1\,, \tag{26}$$

where $\mathbf{c}$ is the beamforming weight vector that produces Koh and Weiss's reference constant-beamwidth beampattern (a periodic sinc). The weights were normalized by using (10) to satisfy the distortionless constraint (4). For the comparison, we set $\theta_{\rm B} = 36^\circ$ since Koh and Weiss's technique does not provide a means to control the beamwidth; their FNBW is fixed at a value that depends on the number of sensors in the array and on the interelement spacing (which is fixed to half of the highest wavelength and is not meant to be adjusted). For this example, their FNBW is approximately 36° – a consequence of their reference beampattern. We now show that even when we design our beamformer to maintain the exclusive FNBW of the competing method, ours outperforms.

The beampatterns using our method and [14] are illustrated in Fig. 2. Both approaches achieve nulls at the interferers' directions, and maintain the distortionless constraint. The beamwidth is constant using the proposed method, but is approximately constant using the competing method. Notice that the beampatterns are asymmetric because the two interferers' directions are not symmetric with respect to the broadside axis. The beamformers' performance measures are displayed in Fig. 3 as a function of frequency. The WNG and DF represent the array gains in white and diffuse noise environments, respectively [19]. The proposed beamformer achieves higher DF and lower sidelobe levels than the competing method, although the WNG is slightly lower. Our method maintains the precise FNBW, unlike [14] where the interferers' directions influence their beamwidth. Our beamformer inherited these positive traits from the CBW subarray while simultaneously nulling the interferers due to the LCMV subarray.

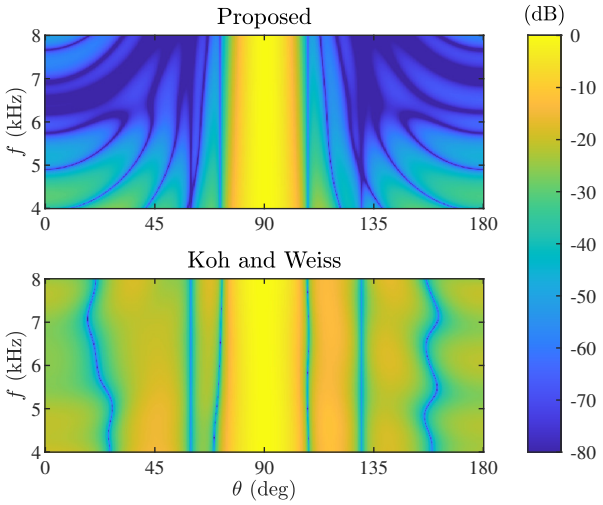

Fig. 2. Constant-beamwidth LCMV beampatterns for $M = 13$, $\theta_{\mathrm{d}} = 90°$, $\theta_{\mathrm{B}} = 36°$, $\theta_1 = 60°$, and $\theta_2 = 130°$.

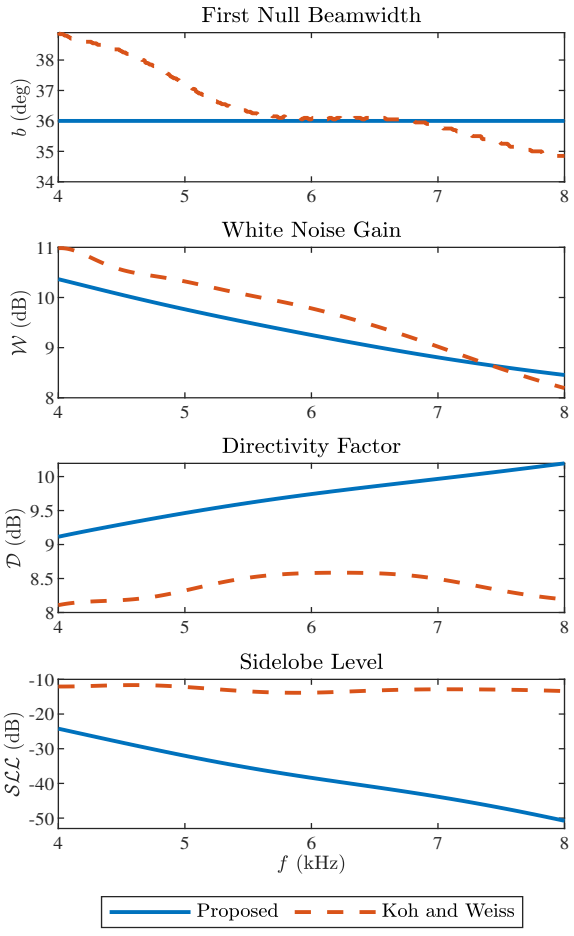

Fig. 3. Performance measures as a function of frequency for the constant-beamwidth LCMV beamformers for $M = 13$, $\theta_{\mathrm{d}} = 90°$, $\theta_{\mathrm{B}} = 36°$, $\theta_1 = 60°$, and $\theta_2 = 130°$.

V. Conclusions

We have proposed a method for designing a constant-beamwidth beamformer that satisfies null constraints. Our method decomposes the problem into two elementary ones and merges them based on the generalized Kronecker product beamforming. Our method offers flexible control over the FNBW, unlike the competing method. Additionally, our method achieves significant sidelobe attenuation, has a high directivity factor, and is simple to implement. Harmonic nesting, together with the proposed spatial tapering, can maintain the constant beamwidth over multiple octaves. Future studies could generalize the method to two- and three-dimensional arrays and beam steering.

References

[1] B. D. Van Veen and K. M. Buckley, "Beamforming: A versatile approach to spatial filtering," *IEEE assp magazine*, vol. 5, no. 2, pp. 4–24, 1988.

[2] H. L. Van Trees, *Optimum Array Processing: Part IV of Detection, Estimation, and Modulation Theory*. John Wiley & Sons, 2004.

[3] W. Liu and S. Weiss, *Wideband Beamforming: Concepts and Techniques*. John Wiley & Sons, 2010, vol. 17.

[4] D. B. Ward, R. A. Kennedy, and R. C. Williamson, "Theory and design of broadband sensor arrays with frequency invariant far-field beam patterns," *The Journal of the Acoustical Society of America*, vol. 97, no. 2, pp. 1023–1034, 1995.

[5] S. Yan and Y. Ma, "Design of FIR beamformer with frequency invariant patterns via jointly optimizing spatial and frequency responses," in *Proc. International Conference on Acoustics, Speech, and Signal Processing*, vol. 4. IEEE, 2005, pp. iv–789.

[6] L. Feng, G. Cui, X. Yu, R. Liu, and Q. Lu, "Wideband frequency-invariant beamforming with dynamic range ratio constraints," *Signal Processing*, vol. 181, p. 107908, 2021.

[7] R. Liu, G. Cui, Q. Lu, X. Yu, L. Feng, and J. Zhu, "Constant beamwidth receiving beamforming based on template matching," in *Proc. IEEE Radar Conference*. IEEE, 2021, pp. 1–5.

[8] T. Long, I. Cohen, B. Berdugo, Y. Yang, and J. Chen, "Window-based constant beamwidth beamformer," *Sensors*, vol. 19, no. 9, p. 2091, 2019.

[9] O. L. Frost, "An algorithm for linearly constrained adaptive array processing," *Proceedings of the IEEE*, vol. 60, no. 8, pp. 926–935, 1972.

[10] K. Buckley, "Spatial/spectral filtering with linearly constrained minimum variance beamformers," *IEEE Transactions on Acoustics, Speech, and Signal Processing*, vol. 35, no. 3, pp. 249–266, 1987.

[11] D. Wolff, Y. Buchris, and I. Cohen, "A directionaly constrained distortionless multistage LCMV beamformer," in *Proc. 2016 IEEE International Workshop on Acoustic Signal Enhancement (IWAENC)*. IEEE, 2016, pp. 1–5.

[12] L. Griffiths and C. Jim, "An alternative approach to linearly constrained adaptive beamforming," *IEEE Transactions on antennas and propagation*, vol. 30, no. 1, pp. 27–34, 1982.

[13] B. R. Breed and J. Strauss, "A short proof of the equivalence of LCMV and GSC beamforming," *IEEE Signal Processing Letters*, vol. 9, no. 6, pp. 168–169, 2002.

[14] C. L. Koh and S. Weiss, "Constant beamwidth generalised sidelobe canceller," in *Proc. 13th Workshop on Statistical Signal Processing*. IEEE, 2005, pp. 283–288.

[15] T. Chou, "Frequency-independent beamformer with low response error," in *Proc. International Conference on Acoustics, Speech, and Signal Processing*, vol. 5. IEEE, 1995, pp. 2995–2998.

[16] W. Yang, G. Huang, J. Benesty, I. Cohen, and J. Chen, "On the design of flexible kronecker product beamformers with linear microphone arrays," in *Proc. International Conference on Acoustics, Speech and Signal Processing (ICASSP)*. IEEE, 2019, pp. 441–445.

[17] J. Kaiser and R. Schafer, "On the use of the I_0-sinh window for spectrum analysis," *IEEE Transactions on Acoustics, Speech, and Signal Processing*, vol. 28, no. 1, pp. 105–107, 1980.

[18] J. Benesty, I. Cohen, and J. Chen, *Array Processing: Kronecker Product Beamforming*. Springer, 2019, vol. 18.

[19] ——, *Fundamentals of Signal Enhancement and Array Signal Processing*. John Wiley & Sons, 2017.